Methanol steam reforming behavior of copper impregnated over CeO_2–ZrO_2 derived from a surfactant assisted coprecipitation route

Dipak Das [a], Jordi Llorca [b], Montserrat Dominguez [b], Sara Colussi [c], Alessandro Trovarelli [c], Arup Gayen [a,*]

[a] Department of Chemistry, Jadavpur University, 700032 Kolkata, India
[b] Institut de Tècniques Energètiques, Centre for Research in Nanoengineering, Universitat Politècnica de Catalunya, 08028 Barcelona, Spain
[c] Dipartimento di Chimica, Fisica e Ambiente, Università di Udine, 33100 Udine, Italy

abstract

A series of ceria-zirconia solid solutions has been prepared by a surfactant assisted coprecipitation method. After impregnation of copper, their activities have been assessed for methanol steam reforming. The results indicate that the compositions with 10 and 15 at.% loading of copper on $Ce_{0.6}Zr_{0.4}O_2$ exhibit maximum catalytic efficiency. Detailed structural analyses reveal high degree of copper dispersion on the ceria-zirconia matrix. In situ XPS studies confirm reduction of surface CuO species with concomitant lowering of Cu-surface atomic composition and increase of carbon. These evidences point to the formation of large aggregates of copper covered with coke that is suggested to be responsible for on stream activity loss. On regeneration, these aggregates break into a mixture of oxidized (Cu^{2+}) and reduced (Cu^0 and Cu^+) copper species showing similar activity to the as prepared catalysts. In general, we have attributed catalytic activity to different proportions of copper components in the various forms of these catalysts.

Introduction

With the increasing pace of modern civilization the energy demand is following an upward trend. The limited sources of fossil fuels, their continuously rising cost and alarming environmental concerns have driven the research into alternative clean sources of energy. Hydrogen energy is regarded as a promising alternative to fossil fuels, since in principle it can be generated from renewable resources such as water [1]. Fuel cells are powerful environment friendly tool for energy production [2], and in particular polymer electrolyte membrane fuel cells (PEMFCs) are suitable for small scale power generation, such as auxiliary power units and portable devices. They require hydrogen as fuel, its storage and transportation becoming a big challenge. Nevertheless, the storage problem can be overcome through the in situ production of hydrogen on demand through the efficient reforming of hydrocarbon

* Corresponding author. Tel.: +91 33 2457 2767; fax: +91 33 2414 6223.
E-mail address: agayenju@yahoo.com (A. Gayen).

[3,4]. The production of fuel cell grade hydrogen containing very low level of CO (<10 ppm) is a challenging issue. Hydrogen can be produced via steam reforming of hydrocarbons, alcohols and ethers. Among these routes, hydrogen production via methanol steam reforming (MSR) has drawn considerable interest in recent years due to several advantages [5]. The MSR reaction (Eq. (1)) takes place along with two possible side reactions, namely methanol decomposition (Eq. (2)) and water gas shift (WGS) reaction (Eq. (3)) [6].

$$CH_3OH + H_2O \rightleftharpoons 3H_2 + CO_2 \quad \Delta H^0 = 49.7\ kJ\ mol^{-1} \tag{1}$$

$$CH_3OH \rightleftharpoons CO + 2H_2 \quad \Delta H^0 = 90.2\ kJ\ mol^{-1} \tag{2}$$

$$CO + H_2O \rightleftharpoons CO_2 + H_2 \quad \Delta H^0 = -41.2\ kJ\ mol^{-1} \tag{3}$$

Though the CO formation can take place either via reverse WGS reaction or via methanol decomposition, most studies have reported its formation exclusively through the former reaction [4,7–9]. Peppley et al. suggested that the major pathway for CO formation is the WGS equilibrium, whereas the methanol decomposition reaction is the less significant one [6]. The selectivity towards primary products CO_2 and H_2 and the secondary product CO depends on the type of catalyst. The Cu(111) model system is more selective towards CO_2 and H_2 while Pd(111) model systems are more selective towards CO and H_2 [10].

Several catalytic systems based on Cu [6,7,11] and Pd [5] have been reported in the literature for MSR; they clearly show that the Cu-based catalysts are highly active and selective at lower temperatures. The commercial MSR catalyst $Cu/ZnO/Al_2O_3$ contains a high loading of Cu and ZnO and a relatively lower amount of Al_2O_3 [12]. The ZnO improves the dispersion and redox properties of copper and is responsible for strong metal support interaction [13,14]. Alumina is shown to have structural and electronic promotional effect on ZnO by inducing lattice defect and increasing its reducibility [12]. In general, the addition of Al_2O_3 leads to the improvement of surface area of the support [11,13]. The incorporation of Al_2O_3 in co-precipitated catalysts was responsible for reduced sintering of copper. But a high concentration of Al_2O_3 also promotes the production of formaldehyde byproduct. With increasing Al_2O_3 concentration MSR activity decreases because it inhibits CuO reduction due to a strong interaction between Al_2O_3 and CuO [11,15,16]. Highly reducing atmospheres is reported to cause a phase change in the catalyst structure that result in sintering. Search for an alternative to ZnO has thus drawn considerable interest in recent years. Addition of ZrO_2 to Cu-based Al_2O_3 supported catalysts has been shown to improve MSR behavior [17–19]. The addition of zirconia also improves the reducibility and dispersion of copper, indicating that ZrO_2 has an effect similar to ZnO. The reducible oxide CeO_2 has been shown to increase the thermal stability of Al_2O_3-supported Cu-catalysts and it also influences the CO conversion through WGS reaction [20]. Moreover, CeO_2 is well known for its high oxygen storage capacity [21]. Partially reduced CeO_2 under reducing environment has been shown to affect the valance state of supported metal [22] and it also produces mobile oxygen, which improves the activity [21].

The CeO_2–ZrO_2 mixed oxide supports can therefore have several beneficial effects on MSR catalysts like improvement of metal dispersion, enhancement of long term stability and, more importantly, resistance against carbon deposition [17,20,23,24]. However, there are very limited reports in the literature emphasizing the investigations on copper based ceria-zirconia systems for MSR activity [7,11,23,25–30]. The ceria-zirconia oxides with varied molar ratio of Ce:Zr have also been shown to be highly effective supports for oxidative steam reforming of methanol [31,32], partial oxidation of methane [33] and ethanol reforming [34].

A large number of methods have been reported in the literature for the preparation of $Ce_xZr_{1-x}O_2$ solid solution like co-precipitation [35,36], sol–gel technique [36,37] and surfactant-assisted route [38–41]. The latter method has drawn considerable interest due to the high surface area and improved thermal stability of the resulting materials [39].

In this work we investigate CeO_2–ZrO_2 supported Cu catalysts for MSR in order to allow a deeper understanding of the key parameters affecting catalytic activity. A series of CeO_2–ZrO_2 oxide supports have been prepared by varying the CeO_2 to ZrO_2 molar ratio via a surfactant assisted coprecipitation method followed by copper loading by incipient wetness impregnation (IWI). A series of studies aimed at the investigation of the effects of copper loading and pretreatment on MSR activity have been carried out. The most promising candidates have been subjected also to continuous ageing treatment (50 h). The MSR activities of the aged catalysts have been subsequently tested. The aged materials have been regenerated through an intermediate in situ oxidation treatment, in order to check the reusability of the catalysts. The MSR reaction has also been monitored through in situ XPS study. Based on these studies, we have proposed an explanation for the MSR behavior exhibited by these catalysts by correlating their activity pattern with the microstructural features obtained from HRTEM studies and the surface information from in situ XPS studies.

Experimental

Preparation of materials

Ceria-zirconia (Ce–Zr) solid solutions, $Ce_xZr_{1-x}O_2$ (x = 0.4, 0.5, 0.6, 0.7 and 0.8), were prepared by a surfactant assisted co-precipitation method. The method involves slow addition of an aqueous solution containing stoichiometric amount of $(NH_4)_2Ce(NO_3)_6$ (Merck, GR, 99%) and $ZrO(NO_3)_2.H_2O$ (Loba Chemie, ZrO_2 assay >44.5%) to an aqueous solution of the surfactant cetyltrimethylammonium bromide (CTAB, Spectrochem, 98%) maintaining [CTAB]/([Ce] + [Zr]) = 1 under stirring condition. The resulting aqueous mixture was stirred further for 0.5 h at room temperature and then aqueous ammonia was added drop wise under vigorous stirring until pH ~ 11. This resulted in the appearance of a yellow-brown precipitate which was further stirred for about 4 h when it was converted to light yellow slurry. After ageing for 12 h the precipitate was centrifuged (Sigma 3–30 K) at 10,000 rpm and washed with deionized water and ethanol several times to ensure the complete removal of the surfactant. Finally, the

precipitate was dried in an oven at 110 °C for 12 h and subsequently calcined in air at 400 °C for 3 h to get the CeeZr oxide material.

The copper loaded ceria-zirconia mixed oxides were synthesized by incipient wetness impregnation (IWI) of an aqueous solution of $Cu(NO_3)_2.3H_2O$ (Merck, GR, 99%) corresponding to the pore volume of the respective supports. After each impregnation, the sample was dried at 110 °C for 12 h and finally calcined at 400 °C for 3 h to obtain the copper loaded CeeZr materials (CueCeeZr). Table 1 lists all the pure as well as copper impregnated materials investigated in this study.

Characterization of materials

The powder X-ray diffraction (XRD) data were collected on a Bruker D8 Advance X-ray diffractometer using Cu Ka radiation (l ¼ 1.5418 Å) operating at 40 kV and 40 mA. The XRD patterns were recorded in the 2q range of 10e100° using Lynxeye detector (1D mode) with a step size of 0.02° and a dwell time of 0.4 s per step and analyzed by ICDD (International Centre for Diffraction Data) database for phase identification. Average particle sizes were calculated from the line-width broadening of the XRD peaks using Scherrer's equation.

The BET surface areas were measured in a TriStar3000 surface area analyzer (Micromeritics). Before each measurement, the samples were degassed at 150 °C in vacuum for 90 min.

Temperature Programmed Reduction (H_2-TPR) experiments were carried out in a Micromeritics Autochem apparatus under a mixture of 5% H_2 in N_2 and heating 40 mg of samples up to 1000 °C at a heating rate of 10 °C min^{-1}. Prior to TPR measurements, the samples were treated for 1 h at 350 °C in air in order to clean the catalyst surface.

The microstructural characterization by High Resolution Transmission Electron Microscopy (HRTEM) was performed at an accelerating voltage of 200 kV in a JEOL 2010F instrument equipped with a field emission source. The point-to-point resolution was 0.19 nm, and the resolution between lines was 0.14 nm. The magnification was calibrated against a Si standard. No induced damage of the samples was observed under prolonged electron beam exposure. All the samples were dispersed in alcohol in an ultrasonic bath, and a drop of supernatant suspension was poured onto a holey carbon-coated grid. Images were not filtered or treated by means of digital processing, and they correspond to raw data.

Surface characterization was done with X-ray photoelectron spectroscopy (XPS) on an SPECS system equipped with an Al anode XR50 source operating at 150 mW and a Phoibos 150 MCD-9 detector. The pressure in the analysis chamber was kept always below 10^{-7} Pa. The area analyzed was about 2 mm x 2 mm. The pass energy of the hemispherical analyzer was set at 25 eV and the energy step was set at 0.1 eV. The charge stabilization was achieved by using an SPECS Flood Gun FG 15/40. The sample powders were pressed to self-consistent disks. The following sequence of spectra was recorded: survey spectrum, C 1s, Cu 2p, Ce 3d, Zr 3d, Cu LMM Auger and C 1s again to check for charge stability as a function of time and the absence of degradation of the sample during the analyses. The data processing was performed with the CasaXPS program (Casa Software Ltd., UK). The binding energy (BE) values were referred to the C 1s peak at 284.8 eV. Atomic fractions (%) were calculated using peak areas normalized on the basis of acquisition parameters after background subtraction, experimental sensitivity factors and the transmission factors provided by the manufacturer. In situ MSR experiments were performed in a reaction chamber connected to the XPS analysis chamber that allowed treatments up to 600 °C under atmospheric pressure and the sample was transferred without exposure to air. The temperature of the sample was measured with a thermocouple in

Table 1 e Nominal composition, name, cell parameter, textural and redox (quantitative analysis of TPR data) properties of pure and copper impregnated ceria-zirconia oxides.

Nominal composition	Name	Cell parameter (Å)	Surface area (m^2 g^{-1})	Pore volume (cm^3 g^{-1})	Pore size (Å)	mL H_2 per g CeO_2	% of CeO_2 red[a]
$Ce_{0.4}Zr_{0.6}O_2$	CZ40	5.337 (3)	110	0.177	58.9	70.1	100
$Ce_{0.5}Zr_{0.5}O_2$	CZ50	5.364 (1)	103	0.167	61.1	65.6	94
$Ce_{0.6}Zr_{0.4}O_2$	CZ60	5.354 (5)	125	0.286	76.2	55.9	80
$Ce_{0.7}Zr_{0.3}O_2$	CZ70	5.384 (2)	117	0.223	60.9	41.9	60
$Ce_{0.8}Zr_{0.2}O_2$	CZ80	5.407 (2)	108	0.209	65.7	27.4	39
Cu (10 at.%)/ $Ce_{0.4}Zr_{0.6}O_2$	Cu10CZ40	5.300 (5)	94	0.162	61.6	58.3	58
Cu (10 at.%)/ $Ce_{0.5}Zr_{0.5}O_2$	Cu10CZ50	5.353 (3)	89	0.201	81.8	46.0	58
Cu (7 at.%)/ $Ce_{0.6}Zr_{0.4}O_2$	Cu7CZ60	5.357 (3)	103	0.127	44.6	38.7	54
Cu (10 at.%)/ $Ce_{0.6}Zr_{0.4}O_2$	Cu10CZ60	5.362 (2)	100	0.166	59.1	44.3	49
Cu (15 at.%)/ $Ce_{0.6}Zr_{0.4}O_2$	Cu15CZ60	5.359 (2)	64	0.230	96.6	51.6	42
Cu (10 at.%)/ $Ce_{0.7}Zr_{0.3}O_2$	Cu10CZ70	5.373 (2)	101	0.232	75.0	41.6	49
Cu (10 at.%)/ $Ce_{0.8}Zr_{0.2}O_2$	Cu10CZ80	5.366 (8)	113	0.192	68.2	36.4	46

[a] % of CeO_2 reduced assuming 100% reduction of CuO to Cu^0 (calculated from TPR @ a temperature of 1000 °C).

contact with the sample holder, which was heated with an IR lamp. The evolution of products during the in situ experiments (0e100 amu) was followed by a mass spectrometer. The gases were introduced by means of mass flow controllers and water and methanol were introduced by bubbling the appropriate amount of carrier gas (Ar) to obtain the desired water/methanol ratio.

Test of reforming activity

The powder materials were pressed at first into pellets of 12 mm diameter applying 10 tons of force exerted by a hydraulic press. For all experiments in our study, the pellets of the sample were crushed and sieved to obtain particle sizes in the range 85e100 mesh. MSR experiments were performed in a continuous-flow fixed-bed down flow quartz reactor (ID ¼ 6 mm) in the temperature range 200e330 °C at atmospheric pressure. In each experiment, 100 mg of sample was packed on a bed of quartz wool in the reactor and was placed in a vertical tube furnace. The reaction was carried out in step temperature programmed mode by thyristor powered Eurotherm PID controller (model 2416) and a K-type thermocouple (Omega) was inserted in the reactor in close contact with the catalyst bed to measure the actual reaction temperature. A premixed methanol (Spectrochem, HPLC grade) and water (Millipore) solution was introduced by a KD100 syringe pump (Cole Parmer) at a rate of 0.4 mL h^{-1}. The liquid was passed through stainless steel tube and traveled a very short distance during which it was evaporated by heating tapes maintained at sufficiently high temperature (>150 °C) to ensure a single phase flow. For all experiments in this study steam/methanol (S/M) ratio was kept constant at 1.1 (mol/mol) using nitrogen as carrier and also as the internal standard. The samples were tested at a gas hourly space velocity (GHSV) of 40,000 h^{-1}. The flow of nitrogen (23.5 mL min^{-1}) through the system was controlled precisely by a Bronkhorst High-Tech B V thermal mass flow controller (model Fe201CB).

All the gas lines were made of stainless steel tubing and were wrapped with heating tapes to ensure that the liquid reactants, methanol and water do not condense in the process lines. After the heating zone the unreacted condensable species were removed in a condenser and the remaining non-condensable species were analyzed by an online Agilent 7890A GC equipped with a polar Porapak Q and molecular sieve 5 Å columns, a thermal conductivity detector (TCD) and a flame ionization detector (FID). The molecular sieve separates all permanent gases while the polar packed column separates all other components. The chromatograph was calibrated using known flow rates of pure gases (CO, CO_2, H_2 and CH_4) with N_2 as the internal standard (though no CH_4 was ever detected in our experiments). All the gases used here were of UHP quality (purity >99.99%) and supplied by Indian Refrigeration Stores and BOC India Ltd., Kolkata. The effluent concentrations of all components were monitored by the TCD. To increase the sensitivity towards CO and CO_2, the FID is associated with a methanizer which converts these gases into CH_4. Since methanol was not introduced into the GC, conversion was calculated by performing a carbon balance.

The methanol conversion (X_{MeOH}) and CO selectivity (S_{CO}) have been defined by the following equations:

$$X_{MeOH} = \frac{n_{CO_2} + n_{CO}}{n_{MeOH}} \times 100 \quad (4)$$

$$S_{CO} = \frac{n_{CO}}{n_{CO_2} + n_{CO}} \times 100 \quad (5)$$

where n_{CO2} and n_{CO} are the flow rates (mol min^{-1}) of CO_2 and CO, respectively in the dry reformate and n_{MeOH} is the flow rate of methanol (mol min^{-1}) in the liquid mixture.

The gas sample from the reactor was analyzed once steady state was reached at a particular temperature, approximately 50 min after reaction. Three gas samples were analyzed at each temperature which gave either same or similar (within 1e2%) conversion values and the last GC data were used as the steady state value. The reproducibility of experimental data was verified by performing catalytic tests under the same reaction conditions and the experimental error was estimated to be within 3%. The equilibrium conversion was calculated using the package software HSC5.1 (Outokumpu). The reforming activity was studied over various forms of the catalyst as listed below.

1. AP: Reforming activity was investigated over as prepared form of the catalyst.
2. oxd400: As prepared catalyst was oxidized in situ in 20% O_2/ N_2, from room temperature to 400 °C at a heating rate of 10 °C min^{-1} and dwell there for 1 h. Then it was cooled to 200 °C in the same flow and finally purged with nitrogen at
   this temperature followed by switch to MSR atmosphere.
3. red400: As prepared catalyst was reduced in situ in 20% H_2/ N_2, from room temperature to 400 °C at a heating rate of 10 °C min^{-1} and dwell there for 1 h. Then it was cooled to 200 °C in this flow and subsequently purged with nitrogen followed by switch to MSR atmosphere.
4. aged: The reforming activity of as prepared catalyst was studied at 250 °C for 50 h followed by cooling in N_2 flow to RT. This form of catalyst has been named as the aged catalyst.
5. regn: The catalyst that underwent an ageing treatment at 250 °C for 50 h was cooled in N_2 to 200 °C and further purged with nitrogen for another 30 min. The catalyst was then oxidized in situ in 20% O_2/N_2, from 200 °C to 400 °C at a heating rate of 10 °C min^{-1} and dwell there for 1 h and cooled in N_2 to 200 °C to regenerate the catalyst. The reforming activity was then tested. The resulting material collected after this cycle of test is defined as the regenerated (regn) catalyst.

Results

Textural properties of CeeZr and CueCeeZr oxides

Table 1 lists the surface area (SA) and the porosity data of all the pure and the copper loaded oxides investigated in this study. The surface areas of pure CeeZr oxides are high and fall in the range 100e125 m^2 g^{-1}, with a maximum in the intermediate composition range CZ60. The impregnation of copper (up to 10 at.%) on the respective CeeZr oxides reduces the

surface area (addition of 15 at.% copper on CZ60 reduced the SA by almost 50%). This is most likely due to blocking of all the smaller pores due to copper impregnation as evidenced from the large increase in the pore size from 76 Å for CZ60 to 97 Å for Cu15CZ60. Interestingly, both the 7 and 10 at.% copper loaded samples showed considerable decrease in the pore size with the concomitant decrease in pore volume. This is possibly due to good dispersion of copper over the larger pores originally associated with the parent oxide support (CZ60).

TPR studies

Fig. 1(a) shows the TPR profiles of the bare ceria-zirconia supports, while in Table 1 the corresponding quantitative analysis is reported. TPR profiles show the presence of two main peaks, one with a maximum at about 380 °C and the other one with a maximum at about 550 °C, in agreement with the literature reports for ceria-zirconia systems [42]. The quantitative analysis is consistent with the well known enhanced reducibility of ceria in presence of zirconia. The effect is more pronounced on higher zirconia loaded samples, and that is evidenced from the complete reduction of cerium oxide in CZ40 (which has the lowest ceria content of all oxides).

Fig. 1(b) shows the TPR profiles of the copper loaded ceria-zirconia samples. A common feature for all the materials is the appearance of a low temperature H_2 consumption peak between 70 and 210 °C that is not observed for the bare supports. This peak is clearly due to the addition of copper that

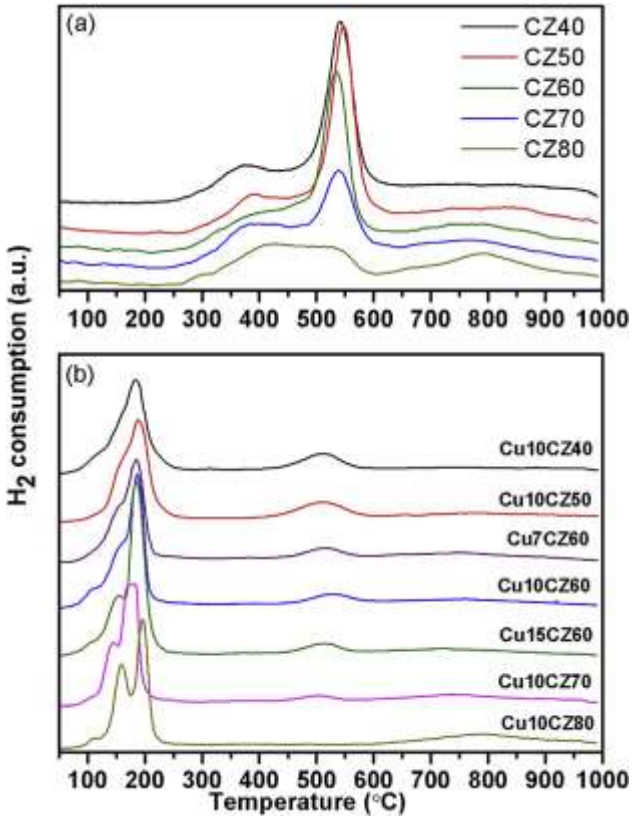

Fig. 1 e TPR profiles for (a) bare ceria-zirconia supports and (b) various copper loaded ceria-zirconia oxides.

not only is reduced to Cu^0, but can also promote CeO_2 reduction through a spillover mechanism widely reported in literature for ceria supported metal catalysts [43,44]. At increasing CeO_2 loading the peak tends to split into three features that are distinguished clearly on Cu10CZ80: the maxima have been related to the reduction of amorphous CuO clusters, bulk CuO interacting with surface ceria and CuO crystallites [45]. These three peaks are typical of ceria-supported CuO, so for this reason it is not surprising that they become evident only for high ceria loading. The peak centered at about 500 °C corresponds to the H_2 uptake observed between 500 and 600 °C for the ceria-zirconia supports. This peak becomes smaller and eventually disappears for high ceria content, as already observed for ceria-zirconia supported materials [42]. The percentage of CeO_2 reduction on copper containing samples has been calculated assuming that on all samples only CuO is present; this is consistent with XRD and HRTEM evidences (see the following sections), and it is further confirmed by XPS analysis of Cu10CZ60 calcined in situ at 350 °C (see Table 2), the same treatment as the one carried out before each TPR experiment. Moreover, the complete reduction of CuO to metallic Cu has been assumed, and we have attributed the extra hydrogen consumption to the reduction of ceria in the support (see Table 1). It is worth noting that the highest CeO_2 reducibility is again observed in the lower Ce-containing samples (i.e., Cu10CZ40 and Cu10CZ50), in agreement with the earlier reports on bare supports. When comparing the same support (CuXCZ60; X ¼ 7, 10 and 15) it can be observed that the amount of reduced ceria decreases with increasing copper loading. This is likely due to the fact that for higher copper dispersion (Cu7CZ60) there is a stronger interaction with ceria that can explain its higher reducibility. The Cu7CZ60 and Cu10CZ60 samples are the most reducible.

Screening of materials for MSR

None of the pure CeeZr oxides exhibits MSR activity in the temperature range investigated in this study; the MSR behavior is therefore reported only for the copper loaded CeeZr oxides. The preliminary reforming experiments are carried out over the 10 at.% copper loaded CeeZr oxides in order to investigate the effect of ceria/zirconia (Ce/Zr) molar ratio for MSR. Fig. 2(a) shows the reforming activity of these samples together with the expected equilibrium conversion of methanol and CO selectivity. The copper impregnated sample with the highest Ce/Zr molar ratio (Cu10CZ80 with the lowest zirconia content of 20 at.%) shows the lowest MSR activity, that increases sharply up to 278 °C (~80% methanol conversion) and reaches a maximum of ~97% conversion at ~330 °C (see Fig. 2(a)). On increasing further the zirconia loading (in steps of 10 at.%), there is a gain in MSR behavior up to 40 at.% of zirconia (i.e., up to Cu10CZ60). It is clearly evident that among the 10 at.% copper loaded CeeZr samples; Cu10CZ60 exhibits the best MSR behavior over the whole range of temperatures investigated here. Specifically, it gives ~73% methanol conversion at 250 °C, ~90% conversion at 275 °C and finally gives 100% conversion beyond 300 °C which is the expected equilibrium conversion value. There is essentially no variation of methanol conversion for 10 at.% copper on CZ50 (Cu10CZ50) and CZ40 (Cu10CZ40; the lowest Ce/Zr ratio

Table 2 – XPS data of pure CZ60 and copper impregnated Cu10CZ60 and Cu15CZ60 catalysts in various forms.

Sample	Name	Position (eV)	Element	% At Conc	% Cu (Cu^0, Cu^b)	% Cu (Cu^{2b})
CZ60	Ce $3d_{5/2}$	882.7	Ce	26.1		
	Zr $3d_{5/2}$	182.0	Zr	9.4	–	–
	O 1s	529.6	O	64.5		
Cu10CZ60	Ce $3d_{5/2}$	882.7	Ce	19.4		
	Cu 2p3/2	932.9	Cu	5.0	42.9	57.1
	Zr $3d_{5/2}$	182.1	Zr	9.4		
	O 1s	529.7	O	66.2		
Cu10CZ60 aged	Ce 3d	882.7	Ce	18.7		
	Cu 2p3/2	933.1	Cu	5.4	20.6	79.4
	Zr $3d_{5/2}$	182.0	Zr	8.7		
	O 1s	529.7	O	67.2		
Cu10CZ60 regn	Ce $3d_{5/2}$	882.6	Ce	21.2		
	Cu 2p3/2	933.0	Cu	6.1	41.3	58.7
	Zr $3d_{5/2}$	182.0	Zr	9.2		
	O 1s	529.6	O	63.5		
Cu10CZ60 calc 350	Ce $3d_{5/2}$	882.7	Ce	23.1		
	Cu 2p3/2	933.8	Cu	5.9	0.0	100.0
	Zr $3d_{5/2}$	181.9	Zr	9.4		
	O 1s	529.6	O	61.7		
Cu10CZ60 MSR 300	Ce $3d_{5/2}$	882.6	Ce	24.2		
	Cu 2p3/2	932.5	Cu	1.4	100.0	0.0
	Zr $3d_{5/2}$	182.2	Zr	9.4		
	O 1s	529.8	O	65.1		
Cu15CZ60	Ce $3d_{5/2}$	882.7	Ce	22.2		
	Cu 2p3/2	933.7	Cu	7.3	3.9	96.1
	Zr $3d_{5/2}$	182.1	Zr	8.9		
	O 1s	529.7	O	61.7		
Cu15CZ60 aged	Ce $3d_{5/2}$	882.7	Ce	20.4		
	Cu 2p3/2	932.8	Cu	7.6	43.9	56.1
	Zr 3d	181.8	Zr	8.4		
	O 1s	529.4	O	63.7		
Cu15CZ60 regn	Ce $3d_{5/2}$	882.7	Ce	16.5		
	Cu 2p3/2	932.8	Cu	8.5	39.8	60.2
	Zr $3d_{5/2}$	182.0	Zr	8.3		
	O 1s	529.7	O	66.8		

studied here) which closely matches with Cu10CZ70 except at higher temperatures (>300 °C). At 300 °C, the Cu10CZ40 sample exhibits ~94% methanol conversion and it remains almost constant at 330 °C. Conversely, the methanol conversion is completed over the Cu10CZ50 sample at 300 °C.

Fig. 2(a) also shows the CO selectivity values for all the samples. The observed CO selectivity values exhibited by all the catalysts lies below the theoretically expected values at equilibrium in the range of temperatures investigated. This can be explained on the basis of the simultaneous occurrence of the water gas shift reaction along with steam reforming [46]. No CO formation is detected at 200 °C (detection limit of our GC is 10 ppm). The Cu10CZ60, Cu10CZ70 and Cu10CZ80 samples exhibit almost similar CO selectivity up to 275 °C. The CO selectivity values of Cu10CZ50 and Cu10CZ40 are found to be higher in the temperature range 230 °C–250 °C, while at 275 °C the CO selectivity is decreased and is similar for all samples (~2.4%). In the temperature range 200 °C–300 °C, the methanol conversion increases sharply with the increase of temperature as expected on the basis of Arrhenius expression. Due to the endothermic behavior of MSR and the reactions leading to CO formation (reverse water gas shift and methanol decomposition), the low or moderate CO selectivity up to 275 °C in the present case indicates that MSR is predominating over the other two. Beyond this temperature, CO selectivity of all the samples increases sharply.

Effect of pretreatment

The activity and selectivity screening carried out on all the samples led us to choose CZ60 as the most effective support for MSR. The effect of pretreatment is therefore studied over Cu10CZ60 catalyst only. Fig. 2(b) shows the reforming activity of Cu10CZ60 in its as prepared, oxd400 and red400 forms as mentioned in the experimental part together with the equilibrium conversion and CO selectivity values which follow the similar trend as noted earlier. The effect of in situ reduction is very severe. There is appreciable difference in conversion between the as prepared and reduced forms of the catalyst up to 300 °C; the oxidized form shows almost similar methanol conversion to that of the as prepared catalyst but with the highest CO selectivity between 230 and 280 °C. Interestingly, the red400 catalyst though shows much lower conversion but it gives a lower CO selectivity than that of the oxd400 catalyst between 220 and 270 °C. There may be a possibility of Cu-sintering (detrimental effect) due to the reductive pretreatment at 400 °C, but to keep the parity in our studies, we choose the thermal treatments at a temperature higher than the

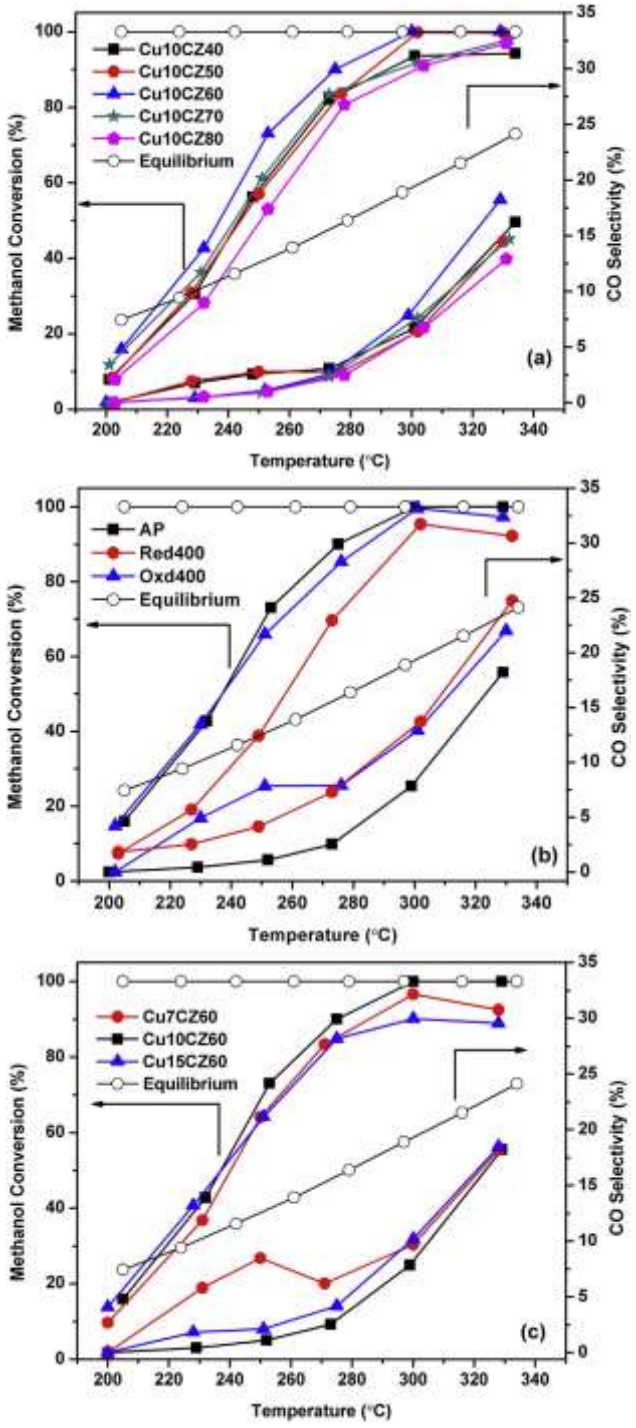

Fig. 2 e Conversion of methanol as a function of temperature at GHSV of 40,000 h^{i1}: (a) over various 10 at.% copper loaded CeeZr oxides, (b) effects of pretreatment on the MSR behavior of Cu10CZ60 and (c) effects of copper loading on the MSR activity of CZ60. The equilibrium conversion and CO selectivity values are also plotted.

maximum temperature studied (330 ° C) for assessing reforming behavior. The highest methanol conversion and the lowest CO selectivity are noted over the as prepared form. The experimental values of CO selectivity of the as prepared Cu10CZ60 catalyst are the lowest at all temperatures suggesting that the WGS reaction occurs easily on the surface as pointed out above. On the contrary, the values of CO selectivity obtained over the oxd400 and red400 forms of the catalyst approaches closely to the equilibrium CO selectivity values beyond 300 °C. We thus used no in situ oxidative pretreatment step in our MSR tests and, unless mentioned, the activity behavior corresponds to that of the as prepared samples.

Effect of copper loading

Fig. 2(c) represents the effect of copper loading on the methanol reforming behavior of CZ60 along with the equilibrium conversion and CO selectivity expected. Among the three copper loadings, the best activity pattern is observed over the 10 at.% Cu-loaded sample that becomes more evident at the higher temperatures. The MSR activity is quite low at 7 at.% Cu-loading over CZ60 (Cu7CZ60) even in the range of temperature 220e270 °C due to the formation of large quantity of CO. The Cu15CZ60 catalyst shows a conversion similar to the Cu10CZ60 up to 230 °C beyond which the recorded activity over the former is lower than that exhibited by the latter. Again, among all the copper loaded CZ60 samples, the as prepared Cu10CZ60 shows the lowest CO selectivity behavior. Such observation led us to select two compositions, namely Cu10CZ60 and Cu15CZ60, to carry out more detailed investigations.

Durability test

To examine the long term stability of the Cu10CZ60 and Cu15CZ60 catalysts, we have studied their time on stream activity in the same reformate composition at 250 °C for about 50 h. Over Cu10CZ60, the initial conversion (~70% of methanol) decreases to ~66% during the first 4 h and then it is decreased steadily to ~61% after 19 h, with a further decrease to 48% of methanol conversion after 50 h on stream (see Fig. 3(a)). The Cu15CZ60 sample shows almost similar trend but the methanol conversion is always lower than the Cu10CZ60 sample; however the extent of activity loss against time is slightly more in this case especially beyond 15 h on stream. Fig. 3(a) shows also the respective CO selectivity patterns of these two catalysts showing that Cu15CZ60 sample has always a lower CO selectivity than the Cu10CZ60 sample. The similarity in the profiles of conversion and the CO selectivity as a function of time on stream implies that the nature of active sites possibly remains the same and only the number of them decreases. From the long term activity patterns the Cu10CZ60 catalyst appears to be the best catalytic formulation for MSR made by the surfactant assisted coprecipitation route reported here.

MSR activity of aged and regenerated catalysts

The continuous decrease of conversion during on stream tests suggests that the aged catalysts will have lower activity behavior than the respective as prepared catalysts. Fig. 3(b) shows the methanol conversion-CO selectivity patterns of the aged and regenerated catalysts Cu10CZ60 and Cu15CZ60 for the whole temperature range along with those of the as

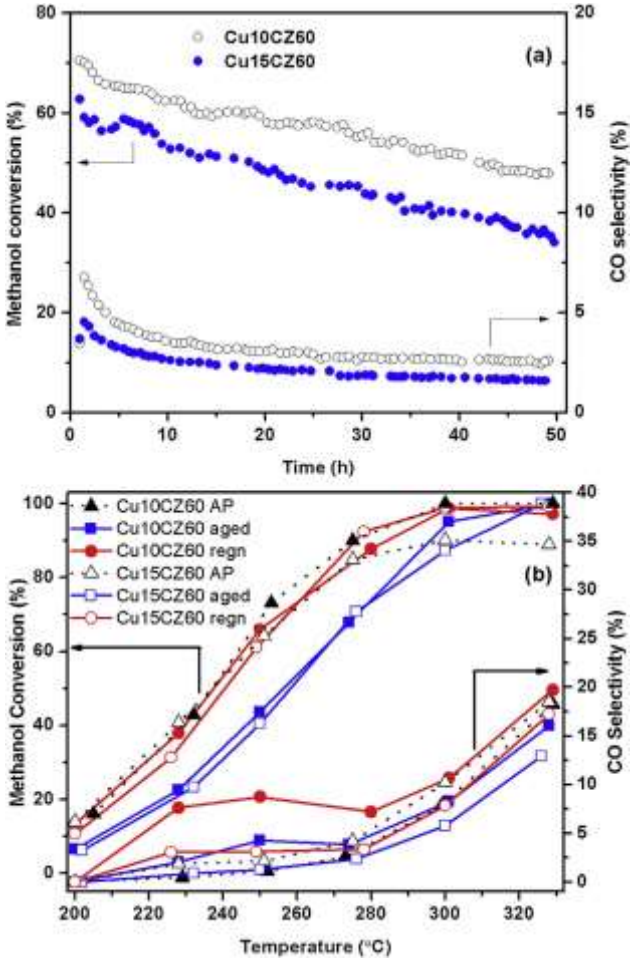

Fig. 3 e (a) Time on stream MSR activity patterns at 250 °C and (b) Effects of ageing (50 h under MSR atmosphere at 250 °C) and regeneration (1 h in 20% H_2/N_2 at 400 °C) on the MSR behavior of Cu10CZ60 and Cu15CZ60 catalysts at GHSV of 40,000 h^{i1}.

prepared catalysts. A comparison of these patterns clearly indicates the appreciable activity loss on ageing. It is also to be noted that the activity pattern of the aged sample Cu10CZ60 is almost similar to that of the in situ reduced catalyst (Cu10CZ60 red400) up to 300 °C (compare with Fig. 2(b)).

The decrease in activity during long term tests is a general observation for this kind of catalytic systems [7,23,25,29]. To investigate in detail the possibility of activity recovery and the catalyst reuse after an intermediate oxidation step, we carried out regeneration tests as described in the experimental section. Fig. 3(b) shows the activity of the in situ regenerated catalysts. It is evident that methanol conversions over the regenerated catalysts not only resemble that of the as prepared catalysts but on regeneration there is a certain gain in conversion beyond 300 °C for the higher copper loaded sample, Cu15CZ60. As expected, the conversion behavior of the regenerated catalyst (Cu10CZ60 regn) closely matches that of the in situ oxidized sample (Cu10CZ60 oxd400 form). Thus, we conclude that Cu10CZ60 and Cu15CZ60 catalysts can be recovered completely as far as methanol conversion is considered by introducing an intermediate oxidation step. But when we compare CO production on the regenerated catalysts, the CO selectivity over Cu15CZ60 regn is found to be lower than over Cu10CZ60 regn.

The turnover frequencies (TOFs) of the various forms of the finalized catalysts have been calculated in two ways. At first, we found a rough estimate of these by considering the mole of hydrogen produced per mole of total copper per second at 250 °C (see Supporting Information for details). However it should be noted that not all the copper is available on the surface for catalytic action as it is evident from the XPS analysis that shows the atomic concentration of copper on the surface to be only 5 at.% for the Cu10CZ60 catalyst (AP form). We thus calculated TOFs considering the XPS surface concentration of copper taking into account the average size of Cu-crystallites from TEM analysis. Doing so, we expect to get a much better and more realistic estimate of TOF. When calculated in this way, the as prepared Cu10CZ60 is found to show the highest TOF of 1.5 s^{-1} and this value is even higher than those obtained over its aged (TOF ¼ 0.8 s^{-1}) and regn (TOF ¼ 1.1 s^{-1}) forms at 250 °C (see Supporting Information). The TOFs calculated similarly for the Cu15CZ60 catalyst are found to be 0.6, 0.4 and 0.5 s^{-1}, respectively for the AP, aged and regn forms. This is in contrast to the XPS surface atomic concentration of copper (see Table 2) that increases from AP to aged and regn samples. This is an indication that not only surface copper atom but also other factors are affecting the reforming activity [18]. On ageing and regeneration there may be decreased interaction between copper and support and some loss of reducibility as well [8,27]. It is also reported that the "quality" of copper surface is an important factor for MSR activity [11,18].

Although methanol conversion recorded for the AP and regn samples are similar, the TOF value of the latter sample is lower than the former. This indicates that in the regn sample reverse WGS and/or methanol decomposition reactions also occur together with the MSR reaction. Thus, the CO selectivity of regn sample is greater than that observed in the AP sample. A similar behavior is also observed in the case of Cu15CZ60 sample but as expected its TOF values are always lower than the Cu10CZ60 sample owing to a higher copper loading in the former. Interestingly, activity recovery on regeneration is higher on the higher copper loaded sample.

XRD studies

The powder XRD patterns of pure CeeZr oxides are shown in Fig. 4(a). All the peaks can be indexed to the cubic fluorite structure. Owing to the smaller size of $Zr^{4þ}$, the peak positions of CeeZr solid solutions are shifted only a little (due to lattice contraction) to higher 2q values with the gradual increase of Zr-loading from CZ80 to CZ40. The average crystallite sizes calculated from full width at half maxima (FWHM) of (111) diffraction lines fall in between 4 and 6 nm. Fig. 4(b) represents the XRD patterns of the CeeZr oxides on impregnation with 10 at.% Cu. The crystallite sizes obtained from Scherrer formula are similar to the pure oxides. No significant CuO related peaks are observed for 10 at.% copper impregnated samples from CZ60 to CZ80 suggesting very good dispersion of copper over all these oxides. The small peaks at 35.5° and 38.7° for the Cu10CZ50 and Cu10CZ40 samples correspond to CuO(002) and

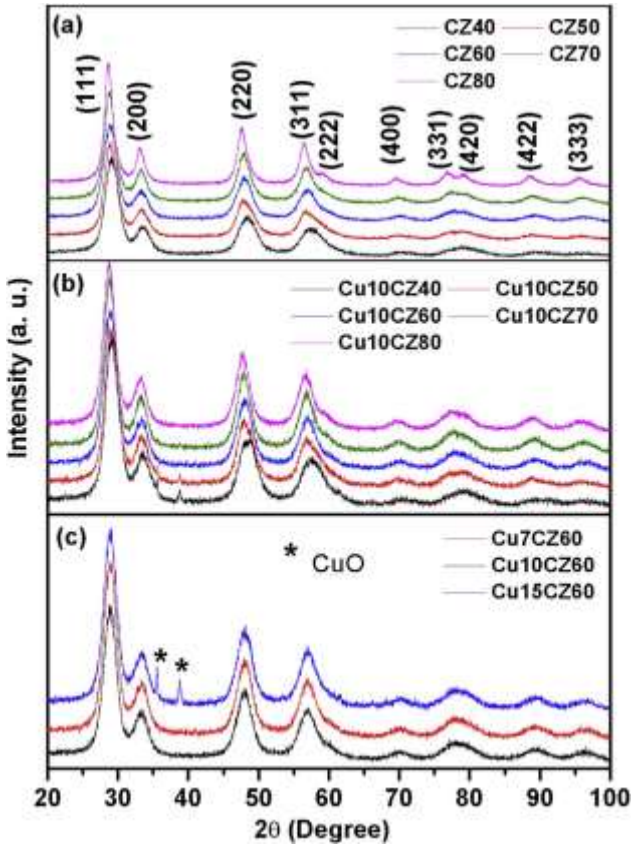

Fig. 4 e Powder XRD patterns of (a) pure CeeZr oxides, (b) various 10 at.% copper loaded CeeZr oxides and (c) different copper loaded CZ60 oxides.

CuO(111) planes suggesting formation of a few large CuO crystallites (of about 25 nm) over these two oxides.

Fig. 4(c) shows the effect of copper loading (7e15 at.%) on CZ60 oxide. As can be seen the CuO related peaks appear when the copper loading is increased from 10 at.% to 15 at.%. No appreciable change in overall crystallite size is evidenced at the highest copper loaded sample. The sizes of CuO crystallites also remain similar.

The least-square refined lattice parameters of the various ceria-zirconia oxides (pure as well as copper impregnated) are also listed in Table 1. As expected the lattice parameter decreases with the gradual increase of zirconium loading in the cubic fluorite structure of ceria for both the pure and the copper loaded oxides. It is to be noted that the cell parameters of CZ50 and CZ60 are quite close to each other. Interestingly, the lattice parameter of the copper impregnated sample is smaller than its pure oxide. When compared with the pure oxide, the impregnation of copper has the effect of reducing the cell parameter as can be ascertained from the systematic decrease from 5.366(8) Å for Cu10CZ80 to 5.300(5) Å for Cu10CZ40. When we look at the cell parameters of CZ60 and various Cu-impregnated samples, the change in lattice parameter remains minimal. The cell parameters of the aged and regn samples of Cu10CZ60 are 5.349(4) Å and 5.352(3) Å, respectively. The corresponding values are 5.348(2) Å and 5.341(2) Å for Cu15CZ60. Note that these values are comparatively smaller than the respective as prepared samples.

TEM studies

We carried out microstructural analysis of only the best support (CZ60) and the corresponding 10 and 15 at.% copper loaded samples in their as prepared, aged and regn forms in order to make a correlation of the MSR activity with the microstructure. Fig. 5(a) shows a general view of the CZ60 support. The support is very homogeneous and mostly constituted by crystallites of about 5e8 nm in size. A detailed lattice fringe image is shown in Fig. 5(b) together with the corresponding Fourier Transform (FT) image. Due to the large number and small size of the support crystallites there are rings in the FT image, which correspond to the fcc structure, fluorite-type. The support particles are perfectly crystalline and well faceted.

Fig. 5(c) corresponds to a general view of the sample Cu10CZ60 in its as prepared form. The appearance is similar to the CZ60 support described above. There are no Cu particles agglomerated. All copper is present as small particles of about 3e4 nm in size. Fig. 5(d) shows two of them. The lattice fringes at 2.53 Å indicate that they correspond to CuO ((002) crystallographic planes).

The general view (not included) of the aged Cu10CZ60 sample is similar to the previous samples, it is constituted by totally crystalline CZ60 particles of about 5e8 nm. A high magnification image is depicted in Fig. 5(e), where a metallic copper particle measuring about 3 nm is identified by the lattice spacing at 2.10 Å ((111) crystallographic planes) in agreement with the XRD findings that show only a signature of metallic copper peak (see slow scan XRD data in Fig. 5(k) in the 2q region 25e55° where copper related phase(s) are expected to be observed). So a portion of the finely dispersed CuO crystallites undergoes reduction in the reforming atmosphere followed by sintering.

The general morphology of the regenerated Cu10CZ60 sample (not included) is also similar to the as prepared sample. At high magnification (see Fig. 5(f)) several CuO particles measuring 4e5 nm are identified in which the lattice fringes at 2.5 and 2.8 Å correspond to (002) and (110) crystallographic planes of CuO, respectively. The XRD pattern of the regenerated sample shown in Fig. 5(k) does not show any peak due to these small CuO crystallites suggesting its excellent dispersion.

From the above HRTEM analysis of the three forms of Cu10CZ60 catalysts, it appears that, initially (as prepared), the sample is comprised by small CuO crystallites well dispersed over the CZ60 support. After ageing, they transform into metallic Cu nanoparticles, and these are reoxidized again into CuO by the regeneration treatment.

The as prepared Cu15CZ60 sample looks very similar to that with less copper content. Fig. 5(g) shows a general view of the sample, again with CZ60 crystallites of about 5e8 nm in size. Fig. 5(h) shows a representative high magnification image, where lattice fringes of CuO at 2.53 Å ((002) crystallographic planes) are identified in addition to those of the CZ60 support particles. The CuO particle measures about 4 nm, similar to the size of CuO in the Cu10CZ60 sample.

The aged Cu15CZ60 sample shows a morphology similar to the aged sample with less copper content (Cu10CZ60) and the copper nanoparticles of about 3 nm are identified under high

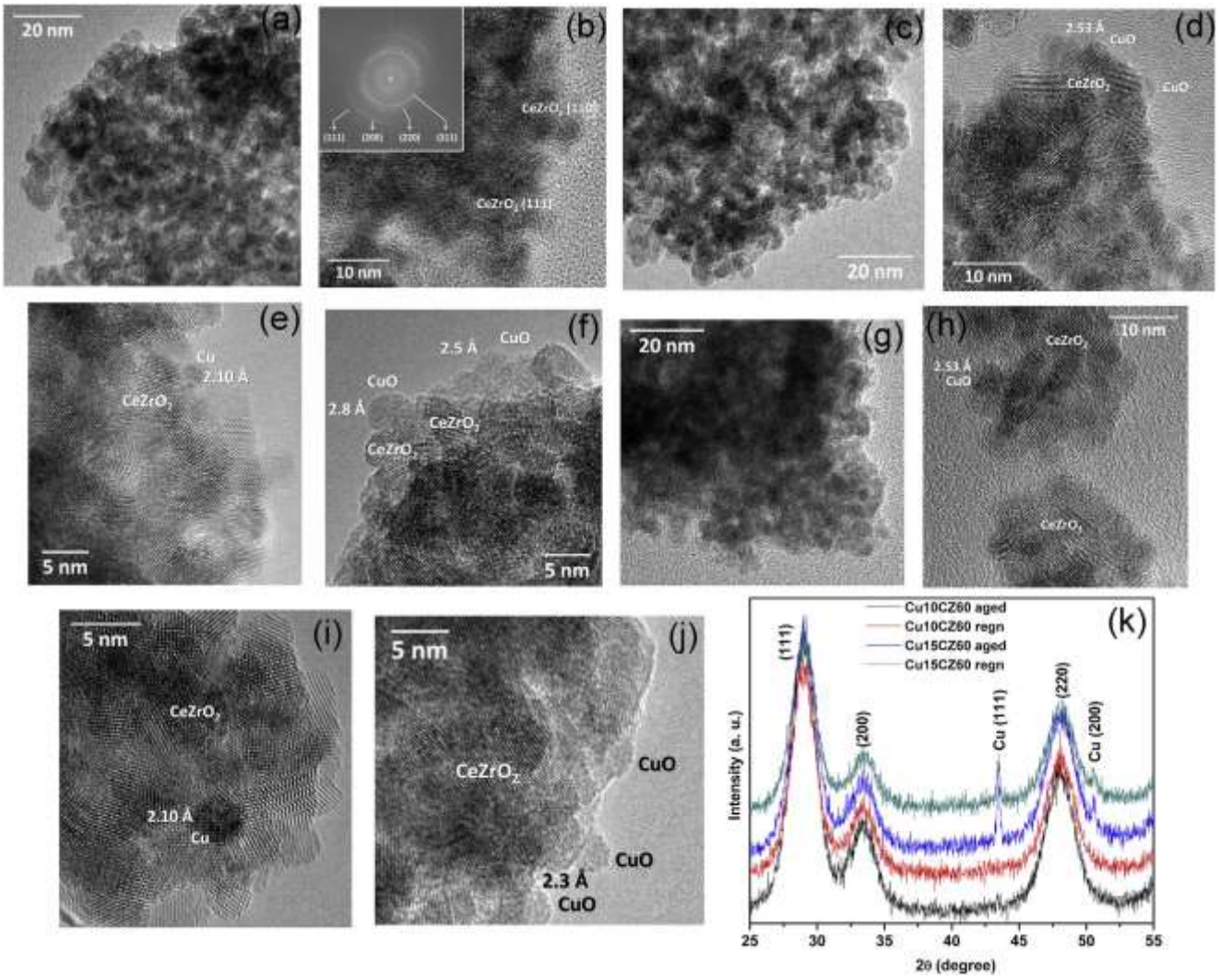

Fig. 5 e TEM images of pure CZ60 (a, b); as prepared (c, d), aged (e) and regenerated (f) samples of Cu10CZ60 catalyst; as prepared (g, h), aged (i) and regenerated (j) samples of Cu15CZ60 catalyst; and (k) slow scan XRD data of Cu10CZ60 and Cu15CZ60 catalysts in aged and regn forms in the 2q range 25e55°.

magnification (see Fig. 5(i), lattice fringes at 2.10 Å correspond to (111) crystallographic planes). The regenerated Cu15CZ60 sample again does not show any difference in morphology with respect to the other samples. Fig. 5(j) corresponds to a high magnification image. Several CuO particles are identified (lattice fringes at 2.3 Å is ascribed to (200) crystallographic planes). No metallic copper could be identified by HRTEM. The XRD data of these two forms of Cu15CZ60 catalyst (see Fig. 5(k)) show narrow peaks due to metallic copper (Scherrer sizes being 38 nm and 31 nm, respectively for the aged and regenerated samples) and the Cu(111)/CZ(111) peak area ratio for both is calculated to be 0.035. Thus metallic copper is also there even after the regeneration treatment and the crystallites are smaller in size than in the aged sample. This is in sharp contrast to the corresponding regenerated sample of Cu10CZ60 where we did not get any signature of metallic copper from XRD analysis.

Therefore, the morphology and composition of samples Cu10CZ60 and Cu15CZ60 look indistinguishable by HRTEM. Both are constituted by very homogeneous CZ60 support particles of about 5e8 nm in size and both contain well-dispersed Cu-based nanoparticles of about 3e5 nm in size. In both cases the fresh samples contain CuO, the aged samples contain metallic Cu, and the regenerated samples contain CuO. However, it should be kept in mind that a limited number of particles can be analyzed in detail by HRTEM, so the presence of CuO in the aged sample or the existence of Cu and/or Cu_2O in the regenerated sample, i.e., co-existence of CuO and Cu and/or Cu_2O cannot be completely ruled out. Although the trend in composition is considered significant since the same phases have been observed independently in both samples.

XPS studies

Apart from the thorough microstructural analysis of the above samples, a detailed XPS analysis was performed to get a deeper insight about the surface state of the materials. The XPS measurements were also performed over Cu10CZ60 under in situ MSR condition. In Table 2 the binding energy

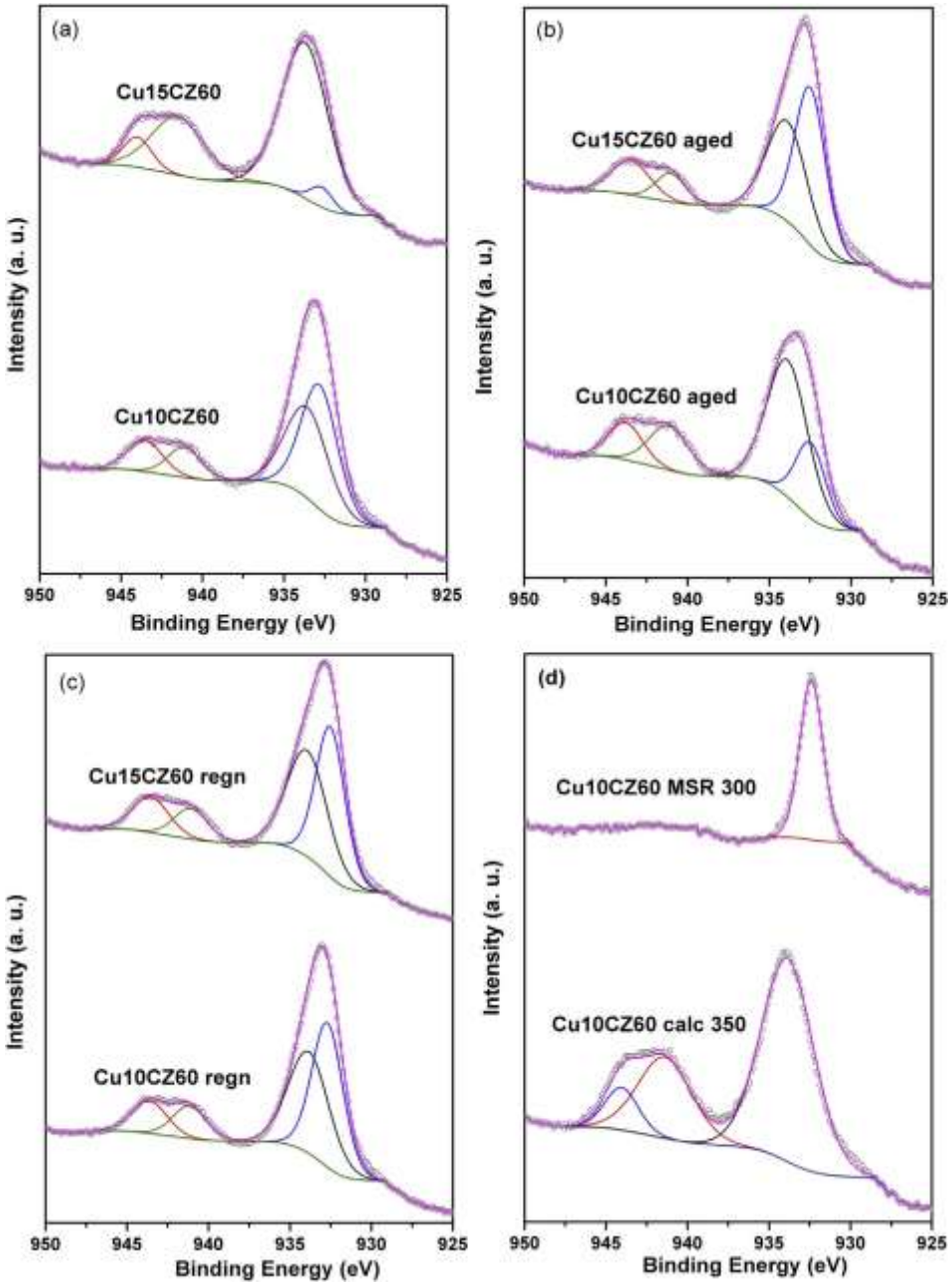

Fig. 6 e XPS of deconvoluted Cu $2p_{3/2}$ regions of (a) as prepared, (b) aged, (c) regenerated samples of Cu10CZ60 and Cu15CZ60 and (d) in situ calcined and MSR samples of Cu10CZ60.

values and surface atomic composition of all samples as well as the amount of oxidized ($Cu^{2þ}$) vs. reduced copper (Cu^0 and $Cu^þ$) are listed.

The bare CZ60 support has a surface Ce/Zr ratio of 2.8, which is significantly higher than the nominal composition (Ce/Zr ¼ 1.5) of the sample, thus indicating a cerium surface enrichment. The O/(Ce þ Zr) ratio is 1.8, which is close to the nominal value of 2. This surface atomic ratio is maintained approximately constant for all the other samples. The ratio between oxide and hydroxyl oxygen atoms is roughly 2:1 and it is also maintained approximately constant.

The amount of copper at the surface in the samples Cu10CZ60, Cu10CZ60 aged and Cu10CZ60 regn is comprised between 5 and 6%, and the amount of copper in the samples Cu15CZ60, Cu15CZ60 aged and Cu15CZ60 regn is little higher, between 7.5 and 8.5%, as expected from the higher copper content in the latter. Interestingly, the Cu surface concentration in the Cu15CZ60 samples is 1.5 times that in the Cu10CZ60 samples, which is exactly the ratio between the nominal copper contents (15/10 ¼ 1.5). This means that the dispersion of copper in both samples should be very similar. This is in agreement with the HRTEM data, where the sizes of CuO and metallic Cu were equal for both samples.

Fig. 6(aec) shows the Cu 2p core level regions of AP, aged and regn forms of the Cu10CZ60 and Cu15CZ60 catalysts. All of them look similar but the results of deconvolution of the

$2p_{3/2}$ region gave varied proportions of copper related components (see Table 2). The as prepared Cu10CZ60 sample contains both oxidized and reduced copper. In particular, the $2p_{3/2}$ signals centered at 934 eV correspond to oxidized copper ($Cu^{2þ}$ species) and that centered at 932.7 eV is due to the reduced copper components ($Cu^{þ}$ and Cu^{0}). The satellite is more pronounced when there is CuO in comparison to other $Cu^{2þ}$ species [47]. Then, it appears that the component at 934 eV may be due to CuO. This component is more intense for the as prepared Cu15CZ60 sample, which exhibits a comparatively stronger satellite signal. The aged Cu10CZ60 sample contains also both oxidized and reduced Cu, but the oxidized component prevails. This could be simply an effect of exposure to air (sample manipulation). By HRTEM, the aged sample exhibited metallic Cu particles. Interestingly, the regenerated Cu10CZ60 sample also contains both oxidized and reduced copper, exactly with the same proportion as the fresh sample. XPS analysis of the fresh Cu15CZ60 sample contains mostly oxidized Cu (see Table 2). The aged Cu15CZ60 sample contains both reduced and oxidized Cu species, and part of the copper is reoxidized after regeneration. These are the same trends as those encountered for the Cu10CZ60 samples.

The methanol steam reforming reaction was also studied by in situ XPS over the Cu10CZ60 sample at S/M ¼ 1.1. The sample was first calcined in situ at 350 °C (sample named as Cu10CZ60 calc 350). In this case, all copper was confirmed to be oxidized to CuO (see Fig. 6(d) and Table 2). The MSR was conducted at 300 °C (sample named as Cu10CZ60 MSR 300), which is the temperature for attaining full methanol conversion (confirmed from the absence of signal at m/z ¼ 31 corresponding to methanol). So we can say that the methanol conversion was 100%, even if the conditions between XPS and flow reactor may differ considerably. Fig. 7(aed) respectively shows the XPS of C 1s, O 1s and Ce 3d along with the Cu LMM Auger spectra of the in situ calcined and MSR samples of Cu10CZ60. The XP spectrum of the sample after MSR shows three distinctive features: (i) Cu is present exclusively in a reduced form, as deduced from the Cu 2p (see Fig. 6(d)) and Auger signals (see Fig. 7(d) in which shape and peak positions indicates the presence of Cu^{0} as well as minor amount of $Cu^{þ}$); (ii) the surface atomic ratio of copper (see Table 2) is decreased sharply from 5.9% (before MSR) to 1.4% (after MSR), meaning that the formation of reduced Cu is accompanied by sintering; and (iii) the amount of carbon on the surface is increased after MSR (see Fig. 7(a)), which means that carbon deposition has occurred during MSR. The O 1s spectra show that the OH like oxygen species is increased on the surface due to contribution from water. When one compares the Ce 3d spectra of the two samples, it is observed that there is decrease in intensity of the satellite peaks suggesting clear reduction of $Ce^{4þ}$ to $Ce^{3þ}$ at the surface during MSR.

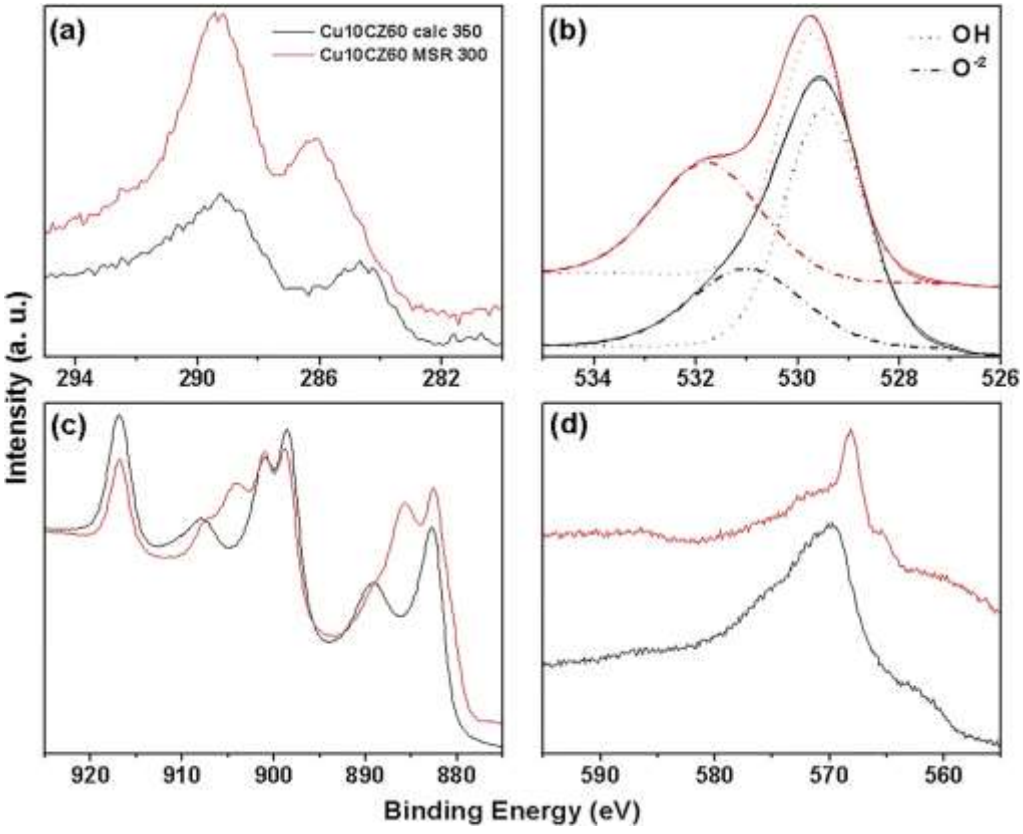

Fig. 7 e XPS of (a) C 1s, (b) O 1s, (c) Ce 3d regions and (d) Cu LMM Auger spectra of in situ calcined and MSR samples of Cu10CZ60.

Discussion

From the results on the copper impregnated ceria-zirconia catalyst systems for MSR, the overall data recorded by XRD, HRTEM and XPS point to the following:

- The fresh CueCeeZr samples are constituted essentially by small crystallites of CuO supported over ceria-zirconia support. By XPS we do see a reduced component at the surface and by HRTEM we only see CuO. So we can speculate that the bulk is CuO and we have some partially reduced copper (Cu^{δ} and Cu^{0}) at the surface.
- Under MSR conditions, CuO undergoes reduction into mainly Cu^{0} (but a minor amount of Cu^{δ} can still be there), which remains as small nanoparticles during initial stages.
- Upon progression of the MSR, the small nano-metal Cu-crystallites sinter to form larger particles and, at the same time, some carbon deposition occurs over the catalysts. We again assume the presence of partially reduced Cu^{δ} phase in the aged catalysts.
- The aged catalysts can be regenerated by oxidation because apart from coke gasification, the large metallic Cu-particles break apart and undergo a kind of rearrangement on the surface to form essentially small CuO nanoparticles together with the two reduced Cu-phases, similar to those present in the fresh samples.

The hierarchical description of surface states proposed above for the various forms of the CueCeeZr catalysts is represented in Fig. 8 where we have assumed occurrence of all the three copper related phases ($Cu^{2\delta}$ as CuO, Cu^{δ} and Cu^{0}) on the CeeZr oxide surface. Note that the presence of partially reduced copper component Cu^{δ} in all the three forms of the catalysts leads to the varied Cu^{δ}/Cu^{0} molar ratio. Presence of $Ce^{4\delta}$ – $Ce^{3\delta}$ redox couple helps to protect a portion of copper from complete reduction to Cu^{0}, maintaining it in δ1 state at the cost of reduction of some amount of $Ce^{4\delta}$ to $Ce^{3\delta}$. This is clearly evidenced from the Ce 3d spectra of MSR 300 sample of Cu10CZ60 justifying our speculation (see Fig. 6(d)). The similar partial reduction of copper has been also recently observed in Cu/CeO_2 catalysts [48]. The partially reduced copper (Cu^{δ}) thus formed is subsequently stabilized by zirconia on the catalyst surface and are in agreement with some studies in the literature for steam reforming reactions up to 300 °C [18,28,49]. We have thus proposed formation of partly reduced CeeZr phase during MSR and in the aged sample in Fig. 8.

The methanol reforming activity of different copper loaded CZ60 samples in their as prepared form can be correlated with the amount of copper loading and its dispersion vis-à-vis the

Fig. 8 e Schematic representation of the catalyst surface states in various forms.

SA and reducibility of the materials. A lower loading of copper (~7 at.%) on CZ60 is not sufficient for the best MSR activity. There was no evidence of CuO peaks in both the Cu7CZ60 and Cu10CZ60 samples suggesting presence of copper in finely dispersed form; on the highest copper loaded sample, Cu15CZ60, a few large CuO crystallites together with smaller ones are present. This sample experienced almost 50% lowering of surface area after impregnation, unlike the 10 at.% copper impregnated sample that experienced a decrease of 20% in surface area (see Table 1). In spite of having the lowest surface area of all the materials, the as prepared Cu15CZ60 sample exhibited comparable methanol conversion to Cu10CZ60 apparently due to a higher copper loading in the former but the TOF's are lower as discussed earlier.

Most of the studies report both Cu^{0} and Cu^{δ} as active species for the MSR and it is the ratio of Cu^{δ}/Cu^{0} that essentially controls the MSR activity behavior [11,27,28]. The metallic copper enhances CO formation through the participation in the mechanism of reverse WGS reaction involving the following steps [50,51]:

$$CO_2 + 2Cu \rightarrow CO + Cu_2O \quad (6)$$

$$H_2 + Cu_2O \rightarrow H_2O + 2Cu \quad (7)$$

In general, the interaction of CO with Cu^{δ} is much stronger than that with the Cu^{0} [52]. This indicates that the presence of Cu^{δ} species on the catalyst surface will ensure the higher reactivity of CO with the available surface oxygen to form CO_2 and thus will reduce the CO selectivity in comparison to the metallic copper species by inhibiting the reverse WGS reaction. Thus, to maintain a low CO selectivity during the MSR, it is necessary not only to have both the reduced copper phases (Cu^{0} and Cu^{δ}) but also a specific range of the Cu^{δ}/Cu^{0} molar ratio on the surface.

The copper containing catalysts are generally prone to deactivation during the course of the reaction. The catalyst deactivation is mainly associated with the thermal sintering of small copper particles leading to a reduction of active surface area [53e55], the change in the oxidation state of copper from its oxidized form ($Cu^{2\delta}$) to the metallic form (Cu^{0}) [4], the variation in Cu^{δ}/Cu^{0} molar ratio [11,26e28] and the deposition of coke on the catalyst surface [56,57]. The continuous activity decrease in our long time on stream tests can be correlated to the formation of the reduced copper phases, namely Cu^{0} and Cu_2O. The formation of more metallic copper with the progress of reaction (on stream activity variation) reduces the Cu^{δ}/Cu^{0} ratio and leads to a decrease in methanol conversion. The as prepared Cu15CZ60 is composed primarily by CuO and is associated with a minor percentage (~4%) of reduced copper phases (see Table 2) and a lower Cu^{δ}/Cu^{0} ratio. Its comparable activity up to 250 °C to that of Cu10CZ60 can be explained as a consequence of the higher copper loading, while the decrease in methanol conversion at higher temperature can be due to further lowering of Cu^{δ}/Cu^{0} ratio because of the Cu^{0} formation via the MSR. On the contrary, over the as prepared Cu10CZ60 the reduced copper species are about 43% (see Table 2). This sample is therefore expected to have more Cu^{δ} component

and obviously a higher Cu^{b}/Cu^{0} ratio than in Cu15CZ60, which is preferred for the best MSR activity. The CO selectivity observed over Cu10CZ60 is thus the lowest one, suggesting it as a better catalyst for the MSR than the Cu15CZ60 in their as prepared forms.

During the regeneration process in the MSR reactor, the metallic copper formed on ageing of Cu10CZ60 is completely oxidized (see Fig. 5(k) where the small peak due to metallic copper present in the aged sample can no longer be detected in the regenerated sample) and this regenerated form gave almost the same methanol conversion of the as prepared catalyst (66% vs. 68.5%) but with a higher CO selectivity than that exhibited by its AP form (8.7% vs. 1.3%). The XPS analysis has revealed the presence of similar amounts of reduced copper components (see Table 2) in both the AP and the regn catalysts of Cu10CZ60. Although there is some possibility of copper oxidation during sample manipulation for XPS study of regn sample, the Cu^{b}/Cu^{0} ratio appears to be lower in the regn sample of Cu10CZ60 than in its corresponding AP sample. This in turn suggests the presence of a larger portion of metallic copper in the regn sample that is likely to be finely dispersed on the support, as no feature of Cu^{0} is attested in the XRD pattern. This is reasonable since the regn sample, after the in situ regeneration and before the characterization, undergoes a cycle of the MSR in which the metallic copper is formed.

Our activity results have also demonstrated that the conversion of the regenerated Cu15CZ60 catalyst is similar to its AP form up to 275 °C and beyond this temperature the methanol conversion is in fact higher and is associated with a lower CO selectivity. The XPS findings of Cu15CZ60 regn have indicated much larger presence (~40%) of reduced copper phases in this sample than in the AP sample. The XRD pattern of the Cu15CZ60 regn (see Fig. 5(k)) sample indeed confirms the presence of metallic copper. Keeping in mind the role of reduced copper components to enhance the methanol conversion maintaining low CO selectivity in the MSR, our findings indicate that on the regenerated Cu15CZ60 catalyst the Cu^{b}/Cu^{0} ratio is likely to be higher than that in its AP form and closely resembles the ratio in as prepared Cu10CZ60 catalyst.

Though there are many studies in the literature on the copper based materials for the MSR as mentioned in introduction, it is difficult to make a direct comparison of all these because of very many differences among the studies especially in reference to the experimental conditions. Thus, we have made an attempt to compare only the differently made ceria-zirconia based copper catalyst systems in the following texts along with two commercial catalysts. The summary of activity data at 250 °C is given in Table 3. Most of the tests are performed at a net oxidizing condition and the S/M ratio varies from 0.75 to 3.1. The direct coprecipitation synthesized CuO loaded over $CuO/CeO_2/ZrO_2$ mixed oxide have been shown to exhibit a high methanol conversion of 80% but with a low GHSV of 16,380 h^{-1} [23]. The time on stream activity data carried out for just 5 h have shown the rate of hydrogen production over this catalyst to suffer a little deactivation. In contrary, a much lower amount of copper deposited over coprecipitation synthesized $Ce_{0.75}Zr_{0.25}O_2$ oxide by the deposition precipitation method have shown ~48% methanol conversion at this temperature when GHSV was 21,000 h^{-1} [25]. But the long term stability of this catalyst investigated at a higher temperature of 300 °C have shown that methanol conversion is decreased continuously up to 10 h and afterward it decreased sharply to near zero. Interestingly, the subsequent addition of gold to it results in the formation of AueCu (1:3) alloy, which eventually leads to an excellent MSR activity [25]. Mastalir et al. have reported preparation of copper loaded CeO_2/ZrO_2 (surface area 102 m^2 g^{-1}) by coprecipitation and the polymer templating route. They have studied the effect of delayed time on stream MSR behavior by continuing the process for a long period as high as 16 days. This treatment revealed the decrease in activity from ~35% to ~17% up to 9 days [7]. The coprecipitation made CuO/ZnO/CeO_2eZrO_2 catalyst is shown to exhibit greater activity and long term stability and the CeO_2eZrO_2 (50:50) support has a greater promotional effect than pure CeO_2, ZrO_2 and Al_2O_3 [29]. The coprecipitation made CuO/ZnO/CeO_2eZrO_2 catalyst prepared by varying the ageing time have shown that the sample prepared after 1 h of ageing exhibits 92% methanol conversion at a GHSV of just 1200 h^{-1} [30]. Ageing for a longer duration resulted in a material showing lower MSR activity. The AueCu/$Ce_{0.75}Zr_{0.25}O_2$ catalyst prepared by the deposition precipitation of AueCu over the coprecipitation made $Ce_{0.75}Zr_{0.25}O_2$ support is reported to exhibit a better MSR behavior than the solegel made support [36]. However, they have not studied the stability behavior of this catalyst. The commercial $CuO/ZnO/Al_2O_3$ catalyst has been reported to exhibit 67% conversion at GHSV of 24,000 h^{-1} [11]. A similar study on a commercial MSR catalyst by Choi and Stenger has shown a good on stream reactivity pattern at a very low space velocity of 1100 h^{-1} [4]. In another study, Kumar et al. have carried out the CO_2 reforming reaction of CH_4 over 5% Ni impregnated on surfactant (CTAB) assisted coprecipitation synthesized $Ce_{0.60}Zr_{0.40}O_2$ showing better the catalytic stability than the corresponding normal coprecipitation prepared sample [39]. In other word, the catalytic activity of the materials is highly sensitive to the synthesis procedure adopted.

Table 3 e Comparison of MSR activity of Cu10CZ60 with the other copper loaded ceria-zirconia oxide materials and commercial catalyst at 250 °C.

Catalyst	GHSV (h^{-1})	S/M	Methanol conversion (%)	Reference
$CuO/CeO_2/ZrO_2$ (8/1/1)	16,380	1.5	80	[21]
Cu (5.18 wt.%)/ $Ce_{0.75}Zr_{0.25}O_2$	21,000	2.0	48	[23]
Au (3.61 wt.%)-Cu (3.4 wt.%)/$Ce_{0.75}Zr_{0.25}O_2$	21,000	2.0	45	[23]
CuO/ZnO/CeO_2eZrO_2 (45/20/35)	1200	1.2	98	[29]
CuO/ZnO/CeO_2eZrO_2 (45/25/30)	1200	1.2	92	[30]
Au (1.5 wt.%)eCu (1.5 wt.%)/$Ce_{0.75}Zr_{0.25}O_2$	21,000	2.0	45	[36]
Cu (15 wt.%)/CeO_2/ZrO_2 (1/1)	e	1.0	35	[7]
$CuO/ZnO/Al_2O_3$ (42/47/11)	24,000	3.1	67	[11]
Commercial catalyst from Sud-Chemie (#EX-2248)	1100	0.75	100	[4]
Cu (4.3 wt.%)/$Ce_{0.6}Zr_{0.4}O_2$ (Cu10CZ60)	40,000	1.1	73	This work

In our present study, we have combined incipient wetness impregnation (for copper) with the coprecipitation (for CeeZr) assisted by a cationic surfactant CTAB and have shown that a much lower amount of copper (4.3 wt.% nominal) impregnated on CZ60 oxide results a catalyst material showing methanol conversion of 73% at 250 °C when GHSV is maintained at 40,000 h^{-1} using a slightly oxidizing condition (S/M ¼ 1.1). Though we have observed a continuous decrease in methanol conversion with time, still the Cu10CZ60 mixed oxide catalyst maintains a methanol conversion of ~65% after 5 h and it is ~48% even after 50 h on stream (see Fig. 3(a)). When this behavior is coupled to the good regeneration characteristics of the material (see Fig. 3(b)), the present catalyst is expected to find a reasonable place in the literature on methanol reforming catalysts.

Conclusions

The steam reforming of methanol for hydrogen generation has been successfully carried out on copper impregnated ceria-zirconia (60:40 molar ratio) catalysts prepared by the surfactant assisted coprecipitation route. Catalysts with 10 at.% and 15 at.% Copper loading on 60:40 atomic ratio of ceria:zirconia were the most active. The two compositions, namely Cu10CZ60 and Cu15CZ60, are shown to be the most promising candidates. The MSR behavior of the catalysts is found to be sensitive to the treatment prior to its use as demonstrated for – as prepared, aged or regenerated catalyst. The best MSR behavior is exhibited by Cu10CZ60 in as prepared form whereas Cu15CZ60 performs better in the regenerated form. However, when the TOF values are considered, the as prepared Cu10CZ60 appears to be the best catalyst for methanol reforming under our reaction conditions. The disparity in reforming behavior of Cu10CZ60 and Cu15CZ60 in the three forms could be attributed to varied proportions of the three copper related phases, namely the oxidized CuO and the reduced Cu metal and Cu_2O, on the ceria-zirconia oxide support leading to differences in Cu^p/Cu^0 molar ratio. During 50 h on stream tests catalysts deactivation takes place, but Cu10CZ60 still retains a conversion of 48% suggesting reasonable stability of the catalyst. Moreover, the regeneration ability of the material enriches further its reforming capability. Finally, we conclude that the catalyst prepared by a combination of impregnation with surfactant assisted coprecipitation routes can go in parallel with the already reported preparation methods for methanol steam reforming.

Acknowledgments

DD thanks CSIR for a research fellowship. Financial support from the Department of Science and Technology, Government of India, by a grant (SR/S1/PC-28/2010) to AG and DST Special Grant to the Department of Chemistry of Jadavpur University in the International Year of Chemistry 2011 is gratefully acknowledged. AG is thankful to Dr. Tapas Kumar Mandal of IIT Roorkee, India for useful discussion on XRD. JL is Serra Húnter Fellow and is grateful to ICREA Academia program (Generalitat de Catalunya). SC and AT acknowledges funding from Italian Ministry under FIRB project RBFR10S4OW and JLl and MD acknowledges funding from Spanish Ministry under MINECO project ENE2012-36368.

references

[1] Cortright RD, Davda RR, Dumesic JA. Hydrogen from catalytic reforming of biomass-derived hydrocarbons in liquid water. Nature 2002;418:964e7.
[2] Rostrup-Nielsen JR. Conversion of hydrocarbons and alcohols for fuel cells. Phys Chem Chem Phys 2001;3:283e8.
[3] Palo DR, Dagle RA, Holladay JD. Methanol steam reforming for hydrogen production. Chem Rev 2007;107:3992e4021.
[4] Choi Y, Stenger HG. Fuel cell grade hydrogen from methanol on a commercial $Cu/ZnO/Al_2O_3$ catalyst. Appl Catal B Environ 2002;38:259e69.
[5] Sà S, Silva H, Brandæo L, Sousa JM, Mendes A. Catalysts for methanol steam reformingeA review. Appl Catal B Environ 2010;99:43e57.
[6] Peppley BA, Amphlett JC, Kearns LM, Mann RF. Methanolesteam reforming on $Cu/ZnO/Al_2O_3$ catalysts. Part 2. A comprehensive kinetic model. Appl Catal A Gen 1999;179:31e49.
[7] Mastalir A, Frank B, Szizybalski A, Soerijanto H, Deshpande A, Niederberger M, et al. Steam reforming of methanol over $Cu/ZrO_2/CeO_2$ catalysts: a kinetic study. J Catal 2005;230:464e75.
[8] Breen JP, Meunier FC, Ross JRH. Mechanistic aspects of the steam reforming of methanol over a $CuO/ZnO/ZrO_2/Al_2O_3$ catalyst. Chem Commun 1999:2247e8.
[9] Agrell J, Birgersson H, Boutonnet M. Steam reforming of methanol over a $Cu/ZnO/Al_2O_3$ catalyst: a kinetic analysis and strategies for suppression of CO formation. J Power Sources 2002;106:249e57.
[10] Gu XK, Li WX. First-principles study on the origin of the different selectivities for methanol steam reforming on Cu(111) and Pd(111). J Phys Chem C 2010;114:21539e47.
[11] Jones SD, Neal LM, Hagelin-Weaver HE. Steam reforming of methanol using Cu-ZnO catalysts supported on nanoparticle alumina. Appl Catal B Environ 2008;84:631e42.
[12] Behrens M, Zander S, Kurr P, Jacobsen N, Senker J, Koch G, et al. Performance improvement of nanocatalysts by promoter-induced defects in the support material: methanol synthesis over Cu/ZnO: Al. J Am Chem Soc 2013;135:6061e8.
[13] Figueiredo RT, Martinez-Arias A, Granados ML, Fierro JLG. Spectroscopic evidence of CueAl interactions in CueZneAl mixed oxide catalysts used in CO hydrogenation. J Catal 1998;178:146e52.
[14] Wang LC, Liu YM, Chen M, Cao Y, He HY, Wu GS, et al. Production of hydrogen by steam reforming of methanol over Cu/ZnO catalysts prepared via a practical soft reactive grinding route based on dry oxalate-precursor synthesis. J Catal 2007;246:193e204.
[15] Chang CC, Chang CT, Chiang SJ, Liaw BJ, Chen YZ. Oxidative steam reforming of methanol over $CuO/ZnO/CeO_2/ZrO_2/Al_2O_3$ catalysts. Int J Hydrogen Energy 2010;35:7675e83.

[16] Huang G, Liaw BJ, Jhang CJ, Chen YZ. Steam reforming of methanol over CuO/ZnO/CeO_2/ZrO_2/Al_2O_3 catalysts. Appl Catal A Gen 2009;358:7e12.
[17] Jeong H, Kim K, Kim T, Ko C, Park H, Song I. Hydrogen production by steam reforming of methanol in a micro-channel reactor coated with Cu/ZnO/ZrO_2/Al_2O_3 catalyst. J Power Sources 2006;159:1296e9.
[18] Agrell J, Birgersson H, Boutonnet M, Melián-Cabrera I, Navarro RM, Fierro JLG. Production of hydrogen from methanol over Cu/ZnO catalysts promoted by ZrO_2 and Al_2O_3. J Catal 2003;219:389e403.
[19] Yong-Feng L, Xin-Fa D, Wei-Ming L. Effects of ZrO_2-promoter on catalytic performance of CuZnAlO catalysts for production of hydrogen by steam reforming of methanol. Int J Hydrogen Energy 2004;29:1617e21.
[20] Zhang X, Shi P. Production of hydrogen by steam reforming of methanol on CeO_2 promoted Cu/Al_2O_3 catalysts. J Mol Catal A Chem 2003;194:99e105.
[21] Maache R, Brahmi R, Pirault-Roy L, Ojala S, Bensitel M. Oxygen storage capacity of PteCeO_2 and Pte$Ce_{0.5}Zr_{0.5}O_2$ catalysts. Top Catal 2013;56:658e61.
[22] Imamura S, Shono M, Okamoto N, Hamada R, Ishida S. Effect of cerium on the mobility of oxygen on manganese oxides. Appl Catal A Gen 1996;142:279e88.
[23] Oguchi H, Nishiguchi T, Matsumoto T, Kanai H, Utani K, Matsumura Y, et al. Steam reforming of methanol over Cu/CeO_2/ZrO_2 catalysts. Appl Catal A Gen 2005;281:69e73.
[24] Nahar G, Dupont V. Hydrogen production from simple alkanes and oxygenated hydrocarbons over ceriaezirconia supported catalysts: review. Renew Sustain Energy Rev 2014;32:777e96.
[25] Pojanavaraphan C, Luengnaruemitchai A, Gulari E. Catalytic activity of Au-Cu/CeO_2-ZrO_2 catalysts in steam reforming of methanol. Appl Catal A Gen 2013;456:135e43.
[26] Pfeifer P, Schubert K, Emig G. Preparation of copper catalyst washcoats for methanol steam reforming in microchannels based on nanoparticles. Appl Catal A Gen 2005;286:175e85.
[27] Szizybalski A, Girgsdies F, Rabis A, Wang Y, Niederberger M, Ressler T. In situ investigations of structureeactivity relationships of a Cu/ZrO_2 catalyst for the steam reforming of methanol. J Catal 2005;233:297e307.
[28] Oguchi H, Kanai H, Utani K, Matsumura Y, Imamura S. Cu_2O as active species in the steam reforming of methanol by CuO/ZrO_2 catalysts. Appl Catal A Gen 2005;293:64e70.
[29] Zhang L, Pan L, Ni C, Sun T, Zhao S, Wang S, et al. CeO_2eZrO_2 promoted CuO/ZnO catalyst for methanol steam reforming. Int J Hydrogen Energy 2013;38:4397e406.
[30] Lei Z, Li-wei P, Chang-jun N, Tian-jun S, Shu-dong W, Yong-kang H, et al. Effects of precipitation aging time on the performance of CuO/ZnO/CeO_2-ZrO_2 for methanol steam reforming. J Fuel Chem Technol 2013;41:883e8.
[31] Pojanavaraphan C, Nakaranuwattana W, Luengnaruemitchai A, Gulari E. Effect of support composition and metal loading on Au/$Ce_{1-x}Zr_xO_2$ catalysts for the oxidative steam reforming of methanol. Chem Eng J 2014;240:99e108.
[32] Pérez-Hernández P, Gutiérrez-Martínez A, Palacios J, Vega-Hernández M, Rodríguez-Lugo V. Hydrogen production by oxidative steam reforming of methanol over Ni/CeO_2eZrO_2 catalysts. Int J Hydrogen Energy 2011;36:6601e8.
[33] Silva PP, Silva FA, Portela LS, Mattos LV, Noronha FB, Hori CE. Effect of Ce/Zr ratio on the performance of Pt/$CeZrO_2$/Al_2O_3 catalysts for methane partial oxidation. Catal Today 2005;107:734e40.
[34] Youn MH, Seo JG, Cho KM, Park S, Park DR, Jung JC, et al. Hydrogen production by auto-thermal reforming of ethanol over nickel catalysts supported on Ce-modified mesoporous zirconia: effect of Ce/Zr molar ratio. Int J Hydrogen Energy 2008;33:5052e9.
[35] Laosiripojana N, Assabumrungrat S. Kinetic dependencies and reaction pathways in hydrocarbon and oxyhydrocarbon conversions catalyzed by ceria-based materials. Appl Catal B Environ 2008;82:103e13.
[36] Pojanavaraphan C, Luengnaruemitchai A, Gulari E. Effect of catalyst preparation on Au/$Ce_{1-x}Zr_xO_2$ and AueCu/$Ce_{1-x}Zr_xO_2$ for steam reforming of methanol. Int J Hydrogen Energy 2013;38:1348e62.
[37] Lin X, Zhang Y, Wang Z, Wang R, Zhou J, Cen K. Hydrogen production by HI decomposition over nickeleceriaezirconia catalysts via the sulfureiodine thermochemical water-splitting cycle. Energy Convers Manage 2014;84:664e70.
[38] Terribile D, Trovarelli A, Llorca J, de Leitenburg C, Dolcetti G. The preparation of high surface area CeO_2eZrO_2 mixed oxides by a surfactant-assisted approach. Catal Today 1998;43:79e88.
[39] Kumar P, Sun Y, Idem RO. Nickel-based ceria, zirconia, and ceriaezirconia catalytic systems for low-temperature carbon dioxide reforming of methane. Energy Fuels 2007;21:3113e23.
[40] Zhao Z, Jin R, Bao T, Lin X, Wang G. Mesoporous ceria-zirconia supported cobalt oxide catalysts for CO preferential oxidation reaction in excess H_2. Appl Catal B Environ 2011;110:154e63.
[41] McGuire NE, Kondamudi N, Petkovic LM, Ginosar DM. Effect of lanthanide promoters on zirconia-based isosynthesis catalysts prepared by surfactant-assisted coprecipitation. Appl Catal A Gen 2012;429:59e66.
[42] Fornasiero P, Monte RD, Rao GR, Ka□par J, Meriani S, Trovarelli A, et al. Rh-loaded CeO_2eZrO_2 solid solutions as highly efficient oxygen enhancers: dependence of the reduction behaviour and the oxygen storage capacity on the structural properties. J Catal 1995;151:168e77.
[43] Fornasiero P, Hickey N, Ka□par J, Dossi C, Gava D, Graziani M. Redox and chemisorptive properties of ex-chloride and ex-nitrate Rh/$Ce_{0.6}Zr_{0.4}O_2$ Catalysts. J Catal 2000;189:326e38.
[44] Giménez-Mañogil J, Bueno-López A, García-García A. Preparation, characterization and testing of CuO/$Ce_{0.8}Zr_{0.2}O_2$ catalysts for NO oxidation to NO_2 and mild temperature diesel soot combustion. Appl Catal B Environ 2014;152:99e107.
[45] Tang X, Zhang B, Li Y, Xu Y, Xin Q, Sen W. CuO/CeO_2 catalysts: redox features and catalytic behaviors. Appl Catal A Gen 2005;288:116e25.
[46] Jeong DW, Na HS, Shim JO, Jang WJ, Roh HS. A crucial role for the CeO_2eZrO_2 support for the low temperature water gas shift reaction over CueCeO_2eZrO_2 catalysts. Catal Sci Technol 2015. http://dx.doi.org/10.1039/c5cy00499c.
[47] Biesinger MC, Lau LWM, Gerson AR, Smart RSC. Resolving surface chemical states in XPS analysis of first row transition metals, oxides and hydroxides: Sc, Ti, V, Cu and Zn. Appl Surf Sci 2010;257:887e98.
[48] Colussi S, Amoroso F, Katta L, Llorca J, Trovarelli A. The effect of ceria on the dynamics of CuOeCu$_2$O redox transformation: CuOeCu$_2$O hysteresis on ceria. Catal Lett 2014;144:1023e30.
[49] Ritzkopf I, Vukojević S, Weidenthaler C, Grunwaldt JD, Schüth F. Decreased CO production in methanol steam reforming over Cu/ZrO_2 catalysts prepared by the microemulsion technique. Appl Catal A Gen 2006;302:215e23.
[50] Ginés MJL, Marchi AJ, Apesteguía CR. Kinetic study of the reverse water-gas shift reaction over CuO/ZnO/A1$_2$O$_3$ catalysts. Appl Catal A Gen 1997;154:155e71.
[51] Matsumura Y, Ishibe H. Selective steam reforming of methanol over silica-supported copper catalyst prepared by soleegel method. Appl Catal B Environ 2009;86:114e20.

[52] Turco M, Bagnasco G, Costantino U, Marmottini F, Montanari T, Ramis G, et al. Production of hydrogen from oxidative steam reforming of methanol I. Preparation and characterization of $Cu/ZnO/Al_2O_3$ catalysts from a hydrotalcite-like LDH precursor. J Catal 2004;228:43e55.

[53] Frank B, Jentoft FC, Soerijanto H, Kröhnert J, Schlögl R, Schomäcker R. Steam reforming of methanol over copper-containing catalysts: Influence of support material on microkinetics. J Catal 2007;246:177e92.

[54] Kurtz M, Wilmer H, Genger T, Hinrichsen O, Muhler M. Deactivation of supported copper catalysts for methanol synthesis. Catal Lett 2003;86:77e80.

[55] Twigg MV, Spencer MS. Deactivation of copper metal catalysts for methanol decomposition, methanol steam reforming and methanol synthesis. Top Catal 2003;22:191e202.

[56] Liu Y, Hayakawa T, Suzuki K, Hamakawa S, Tsunoda T, Ishii T, et al. Highly active copper/ceria catalysts for steam reforming of methanol. Appl Catal A Gen 2002;223:137e45.

[57] Agarwal V, Patel S, Pant KK. H_2 production by steam reforming of methanol over $Cu/ZnO/Al_2O_3$ catalysts: transient deactivation kinetics modeling. Appl Catal A Gen 2005;279:155e64.